Nucleation and evolution of the Au-induced 5×2 structure on vicinal Si(111)

J. D. O'Mahony* and J. F. McGilp
Department of Pure and Applied Physics, University of Dublin, Trinity College, Dublin 2, Ireland

C. F. J. Flipse,† P. Weightman, and F. M. Leibsle
Physics Department and Interdisciplinary Research Centre in Surface Science, University of Liverpool, Liverpool L69 3BX, United Kingdom

(Received 20 July 1993; revised manuscript received 14 August 1993)

Topographical changes on vicinal Si(111) have been followed as a function of submonolayer Au coverage. Nucleation at step edges leads to subsequent growth of a single-domain overlayer of the Au-induced 5×2 structure. Phase boundaries between step, 7×7 and 5×2 regions have been studied, as well as the detailed structure of the step and 5×2 regions. Gradual changes in facet angle on the surface occurred, driven by 5×2 terrace growth. An inhomogeneous coverage of Au was observed, with a pattern extending over distances on the order of micrometers, indicating large-scale surface diffusion of both Au and Si atoms.

I. INTRODUCTION

Gold overlayers on silicon have been extensively studied for many years with a variety of surface analysis techniques.[1–31] In recent years, much of this has been driven by the relevance of this system to the microelectronics industry. Gold growth proceeds differently on Si depending on the crystallographic orientation and temperature of the substrate.[8] The Si(111)-Au system in particular is rich in structure for Au coverages in the monolayer regime,[1–5] where stable structures precede the Au-Si intermixing that occurs for higher coverages.[6] For Au condensation at substrate temperatures above 400 °C,[2] or alternatively on annealing after room-temperature growth, the first ordered overlayer to be formed beyond the clean Si(111)7×7 reconstruction generates a 5×1 low-energy electron diffraction (LEED) spot pattern with second-order diffuse streaks. This "pseudo-5×1" or "5×2" pattern persists for Au coverages in the 0.1–0.5-monolayer (ML) range, with 1 ML corresponding to 7.84×10^{14} Si atoms per cm^2, the atomic density of the upper atoms in the bulk-terminated Si(111) surface bilayer.

Early studies of the nucleation of the 5×2 superstructure by Osakabe *et al.*,[5] using reflection electron microscopy (REM), showed that preferential nucleation occurred at step edges on the Si(111) surface. The structure was also seen to undergo a first-order phase transition to a 1×1 structure at 750 °C, almost 100 °C below the 7×7 to 1×1 phase transition observed on clean Si(111).[32] Detailed examination of Au growth was continued by Ichikawa, Doi, and Hayakawa[10] using microprobe reflection high-energy electron diffraction (microprobe RHEED). The presence of steps on their singular Si substrates was seen to have a strong influence on the nucleation of the Au overlayer. The bulk-terminated Si(111) surface, as well as its 7×7 reconstructed surface, possesses $2\pi/3$ rotation symmetry. Accordingly, upon Au deposition, three equivalent domains of 5×2 row growth are possible, with rows running in the three equivalent $\langle\bar{1}10\rangle$ directions. Ichikawa, Doi, and Hayakawa[10] found that, on singular surfaces, single domains of the 5×2 structure grew along the length of any step edges present, while all three possible domains nucleated on flat terraces. High-resolution REM was applied dynamically to the problem by Tanishiro and Takayanagi,[16] where the growth of the 5×2 was considered to have proceeded across terraces above and below the nucleation step. The 2× periodicity always ran along the step edge, and growth was observed to be faster in that 2× direction. Analysis of terrace widths implied a considerable displacement of Si atoms during the 5×2 formation, with only about 60% of the original surface Si atoms remaining in the 5×2 areas. Step-edge motion was observed by Tanishiro, Yagi, and Takayanagi,[20] again using REM, with steps moving towards the lower terraces during Au growth. By their analysis, the excess Si atoms displaced during the 5×2 growth were required to migrate towards the lower step edges in order to explain the perceived step motion. In the analysis of scanning tunneling microscopy (STM) data by Hasegawa *et al.*,[26] a 5× reconstruction was postulated to occur in the Si substrate itself on deposition of very small quantities of Au. More recently, *in situ* STM studies during the growth process have reaffirmed 5×2 growth both above and below the nucleation step.[28]

As mentioned above, three 5×2 domains can occur in the three equivalent $\langle\bar{1}10\rangle$ directions. However, if a surface is used with a small, specifically chosen, misorientation with respect to the [111] normal, then a single domain can be forced to dominate by virtue of the increased density of steps and their subsequent influence on nucleation and growth.[12,13,30,33,34] An offcut from [111] towards $[11\bar{2}]$ creates step edges in the $[\bar{1}10]$ direction, which force the rows in that direction to preferentially nucleate, and produces a single domain system. The elimination of cross-domain interference can be a powerful tool in simplifying growth studies,[12,13] and has been employed here.

The microscopic detail of the 5×2 structure has at-

tracted considerable attention in its own right. In the mid-1970s, an elegant examination by Lipson and Singer[3] demonstrated, using an optical analogue, how the observed pseudo-5×1 LEED pattern could be generated from rows of 5×2 units if the rows were incoherent with respect to each other in the direction along their length. In 1977, Le Lay and Faurie[4] proposed a simple model of the system involving rows of Au atoms above the ideal Si(111) surface, but later studies, such as ion scattering by Yabuuchi *et al.*[7] and by Huang and Williams,[14] and x-ray standing wave analysis by Berman, Batterman, and Blakely,[15] produced conflicting models. Despite the lack of consensus as to the registry of the Au atoms with respect to the Si lattice, all the early models had in common an intuitively simple Au-row structure and ideal Si(111) surface. More recently, RHEED analysis of the changes in the surface structure upon Li adsorption by Daimon *et al.*[21] hinted at a much more complicated atomic arrangement than had hitherto been considered. The recent STM results of Baski, Nogami, and Quate[18] and Hasegawa *et al.*[22] reinforced those conclusions. To date, no model enjoys complete accord with recent STM results[30] which revealed, with atomic resolution, the details of the Au-row structure. There, it was conclusively shown that the structure is indeed made up of incoherent 5×2 rows, with the 2× periodicity along the length of the row. That work is reported in more detail here, together with an analysis of the topographical changes which occur during the initial stages of Au deposition, up to the completion of the Si(111)-5×2-Au structure.

II. EXPERIMENT

The Si samples used here were from a single wafer, cut 4° off the [111] axis towards the high-symmetry [11$\bar{2}$] direction, boron-doped, *p* type, and with a resistivity in the range 5–25 Ω cm. Samples were initially cleaned in ethanol in an ultrasonic bath, dried in a stream of nitrogen, and then mounted on a carousel sample holder in the main chamber of the STM system. The chamber was equipped with LEED-Auger diagnostics, and had a base pressure better than 1×10^{-8} Pa. Sample heating was by means of electron bombardment of the rear of the sample and all temperatures were measured by optical pyrometry. Samples were first degassed at 800 °C for 24 h to ensure good pressures during high-temperature annealings. Initial flashing to 1050 °C for 30 s was sufficient to clean the samples of their native oxide layers and produce a sharp 7×7 LEED pattern. Auger electron spectra showed no detectable surface contamination. STM confirmed the cleanliness of the samples. Samples were then flashed to 1280 °C for 20 s and rapidly quench-cooled through the formation temperature of the 7×7 structure. The treatment was then repeated, producing a regular array of single steps.[35] [Single steps on the ideal Si(111) surface was defined as being 3.135 Å in height, the distance between the first and second bilayer.] Deposition of Au onto this surface was by means of a Knudsen cell evaporator whose deposition rate was calibrated by both quartz-crystal oscillator and Auger electron spectroscopy.[4] Gold was deposited onto Si samples which were held at 600 °C, and then cooled to room temperature after deposition. LEED patterns were checked after deposition. After heat treatments, samples were allowed at least 2 h to cool before STM images were taken, so as to minimize thermal drift. Because of the restricted field of view of the STM, it is important to verify that any effects seen are truly global. Images reported here were typical of what was found in widely separated areas across the sample surface.

III. RESULTS

Figure 1 shows a typical STM image of the ordered clean metastable Si surface used as the substrate for Au growth. Analysis of such topographs produced a mean step separation of 43±12 Å. The average step density $S(\theta)$ can be expressed as $S(\theta)=(\tan\theta)/h$, where θ is the offcut angle, in this case 4°, and h is the step height. For ideal single-height steps, this gives a step separation of 44.8 Å, in good agreement with the direct measurements. Single-height steps were also verified by direct STM measurement. This was consistent with the split-spot LEED pattern seen during, and after, cooling of the sample. The method employed in generating this specific substrate structure has been reported in detail elsewhere.[35]

The initial Au deposition studied was estimated as 0.1 ML. Together with the 7×7 LEED pattern, a weak single domain pseudo-5×1 LEED pattern was obtained, signifying the presence, in small proportions, of a phased arrangement of 5×2 structures on the surface. The surface, as seen by STM, was inhomogeneous, indicating a high degree of nonuniformity in the Au-atom distribu-

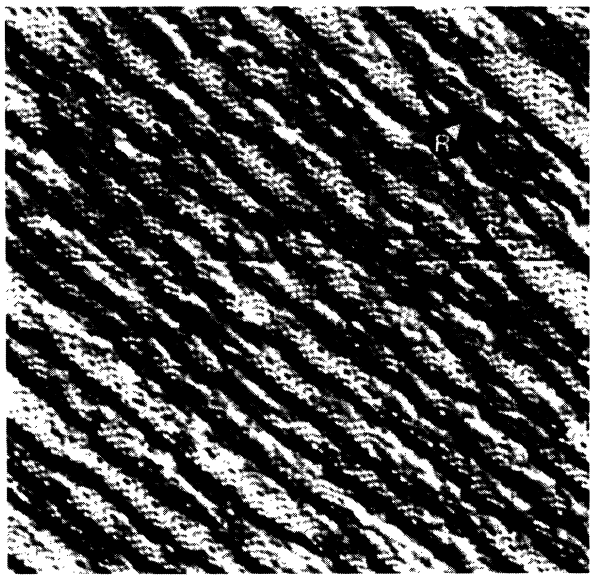

FIG. 1. A 600 Å×600 Å STM topograph of a vicinal Si(111) cut 4° off the [111] towards [11$\bar{2}$]. The surface was produced by flashing the sample twice to 1280 °C for 20 s, followed by quench cooling (Ref. 35). The arrow, labeled *R*, indicates rising step edges in the [$\bar{1}\,\bar{1}$2] direction. The tunneling current was 1 nA for a sample bias of +2 V. The image is nine point smoothed and differentiated to highlight the step edges.

tion. Topographs showed that the regular surface of Fig. 1 had been transformed, and now exhibited flat composite terraced areas, typically about 120 Å in width, separated by wider faceted regions of steps. Figure 2(a) details the terrace regions, while Fig. 2(b) shows the stepped regions on this surface. The composite terraces were regular, but inhomogeneous, consisting of a section of 7×7 reconstruction and a section of 5×2 reconstruction in roughly equal widths. These reconstructions were sharply bounded along the [$\bar{1}$10] direction. The 5×2 region was bounded on one side by the 7×7 terrace section and on the other by a region of *rising* steps, with the 2× periodicity running along the step edges. The 7×7 region was bounded on one side by the 5×2 region and on the other by a region of *falling* steps. Increased ordering along step edges, even in clean areas of the substrate, was apparent in the stepped areas, as seen in Fig. 2(b), with the step edges running sharply through corner hole structures in the [$\bar{1}$10] direction. Some 5×5 Si reconstructions at the step edges were also found, while none were observed on the clean substrate. The average step density, $S(\theta)$, in the stepped areas of Fig. 2(b) was larger than that found on the clean vicinal substrate of Fig. 1, but the same step height was maintained, indicating that these faceted regions were now of steeper offcut from the [111] direction. The flat terraced regions, when interleaved with the faceted regions, compensated for the local changes in vicinality, allowing the global structure to maintain the average 4° offcut. The boundary between the 5×2 and 7×7 regions on these terraces appeared from the STM to be a step upward from the 7×7 to the 5×2.

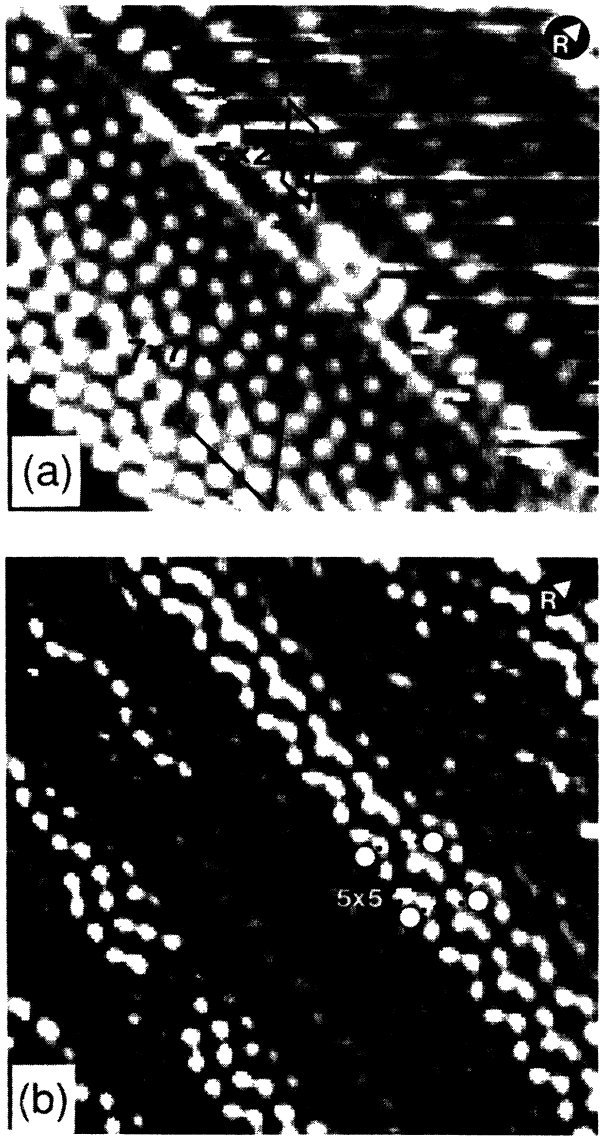

FIG. 2. (a) 120 Å×140 Å STM topograph of a small composite terrace of 7×7 and 5×2 reconstructions found after an initial deposition of 0.1 ML of Au, as detailed in the text. The unit cells are indicated. The two reconstructed regions share a sharp boundary in the [$\bar{1}$10] direction. The tunneling current was 1 nA for a sample bias of +2 V. (b) Enhanced step-edge ordering after initial deposition of ~0.1 ML of Au under the tunneling conditions used in (a). At step edges, small regions of the 5×5 reconstruction can now be found. The step edges run through the corner holes in the [$\bar{1}$10] direction. *R* indicates the rising step-edge direction.

Figure 3(a) shows a 80-Å-square STM topograph of the single domain Si(111)5×2-Au reconstruction taken at −0.4 V sample bias and 1.2 nA tunneling current, while Fig. 3(b) shows the same region at opposite sample bias. The row incoherence, or slippage, is indicated by *S* in Fig. 3(a). Also indicated is a bright feature *P*, previously termed a "protrusion" in the work of Baski, Nogami, and Quate,[18] which is seen here to randomly occupy a site repeated at intervals of 4*a* along the rows in the [$\bar{1}$10] direction, where *a* is the surface translation vector for the Si(111) surface of 3.84 Å. Simultaneous scans of such regions at opposite sample bias always revealed the protrusion features. However, it was found that the resolution of all other features was highly dependent on the tunneling parameters used, as a comparison of Figs. 3(a) and 3(b) clearly shows, indicating substantial structure in the density of states being probed at these positions.

Figure 4 is an expanded view of the repeating units of Fig. 3(a), under the same tunneling conditions as that figure. The repeating units are a series of Y-shaped structures lying side by side with the arms of each Y made up of the paired features (1, 2) and (1*A*, 2*A*), and feature 3 forming the tail. Also in evidence are weaker features labeled 4 and 5. Protrusion feature *P* then occupies a site between the arms of adjacent Y units. Its presence at that site is seen to enhance the brightness of the nearby features (1, 2) and (1*A*, 2*A*). Figure 4 indicates that features 1, 1*A*, 2, 2*A*, and 3 have a strong clustering tendency, while features 4 and 5 appear to interact to a lesser degree with the Y cluster and are more localized.

A further 0.1 ML of Au was deposited on the surface represented by Figs. 2(a) and 2(b). This produced an estimated total Au coverage of 0.2 ML. LEED again showed the single domain pseudo-5×1 pattern, though stronger than before. The composite terraces were seen to increase in width to between 300 and 400 Å, maintaining roughly the same ratio of 5×2 to 7×7 areas. The intervening step regions showed further ordering along the

step edges in the [$\bar{1}$10] direction. The presence of the feature *P*, as labeled in Fig. 4, increased as the Au coverage progressed,[30] though Baski, Nogami, and Quate[18] did not observe this. The boundary between the 5×2 and 7×7 regions was again well defined and sharp, with the same transition line detail along the [$\bar{1}$10] direction. Figure 5 shows the boundary region between these reconstructions, with the tail feature (feature 3) of the 5×2 cell marked for clarity. The dimerlike features are shown by black dot pairs. This narrow boundary strip can also be seen in detail, labeled *B*, in Fig. 3(a).

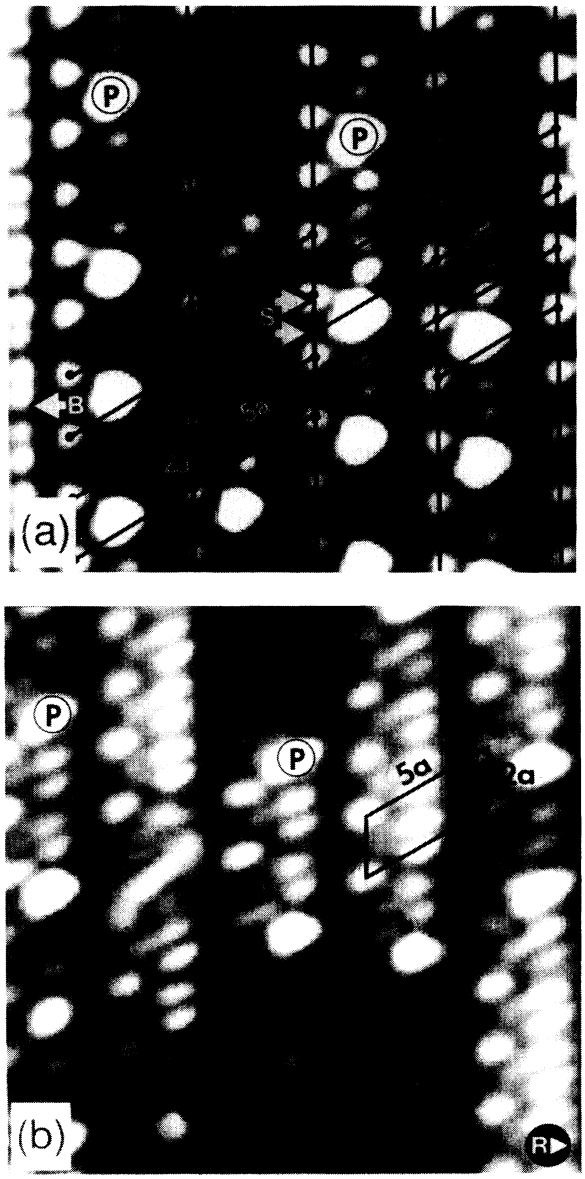

FIG. 3. (a) An 80-Å-square STM topograph taken at −0.4 V sample bias and 1.2 nA tunneling current showing the single domain 5×2 Au-induced reconstruction on Si(111). The slippage of rows (Ref. 3) is indicated by *S*. Large bright areas, termed "protrusions" (Ref. 18) and labeled *P*, occur at sites spaced no closer than 4*a* in the [$\bar{1}$10] direction [*a* is 3.84 Å on the Si(111) surface]. The boundary line between the 5×2 and 7×7 reconstructions is indicated by *B*. (b) The same area as above imaged at sample bias +0.4 V and tunneling current 1.2 nA.

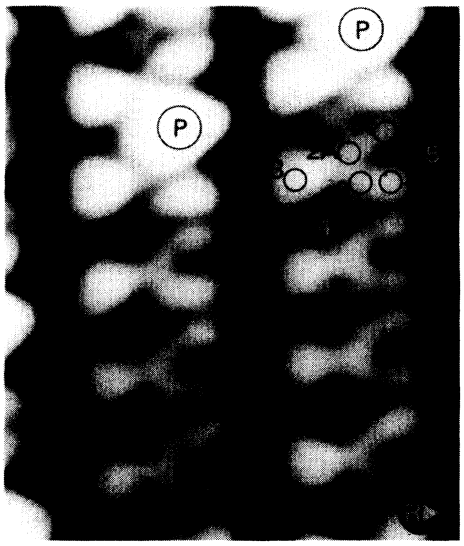

FIG. 4. A 35 Å×40 Å image of the slightly skewed Y structure unit seen in the filled states of the 5×2 rows. The topograph was taken at −0.4 V sample bias and 1.2 nA tunneling current. The main repeating features are labeled and *R* is the rising step-edge direction.

At an estimated total coverage of 0.5±0.1 ML, saturation appeared to be reached for the 5×2 structure. (At coverages above this value, LEED indicated the beginnings of the $\sqrt{3}\times\sqrt{3}R30°$ superstructure which follows the 5×2 reconstruction.) Figure 6 shows the highly or-

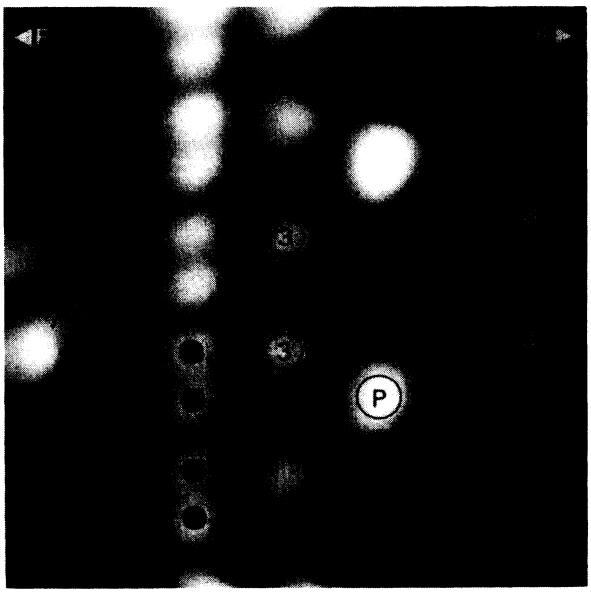

FIG. 5. The detail of the boundary area, shown here in a 40-Å-square image. The boundary line itself is indicated with black dots. These structures appear to be dimerized. The dimer centers are spaced 2*a* apart, the distance between two tail features (3) as labeled in Fig. 4. Rising and falling step-edge directions are indicated, as is a protrusion feature. This image, measured at 1.2 nA and −0.4 V sample bias, has been differentiated to highlight the main features of interest.

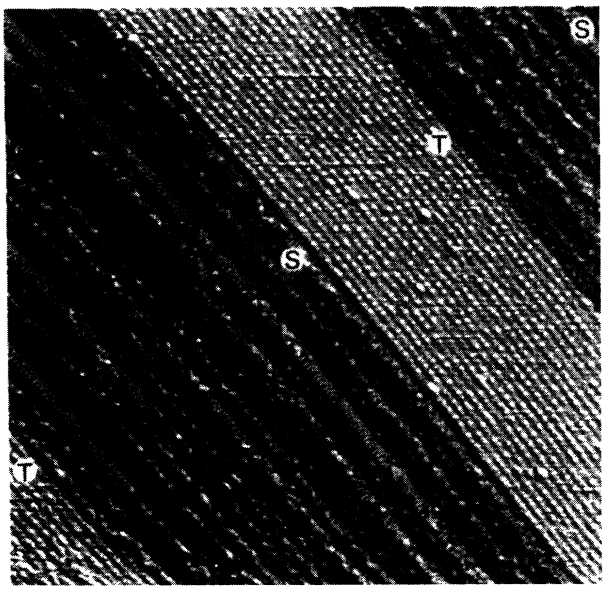

FIG. 6. A topograph measuring 1000 Å square showing a surface with regular saturated terraces (T) consisting only of the 5×2 reconstruction, separated by stepped regions (S). The boundary between these regions along the [$\bar{1}$10] direction is seen to be very regular and sharp. The image has been differentiated and nine-point smoothed.

dered system which exists at saturation. A long-range pattern has been established, with the previously composite terraces now exhibiting the rows of 5×2 reconstruction alone, the 7×7 having been completely eliminated. This was confirmed by LEED which showed only a sharp, low background, single domain, pseudo-5×1 pattern. The saturated terraces of 5×2 in Fig. 6 (labeled T) are bounded by highly ordered regions of bunched single steps (labeled S). The 5×2 regions do not, in general, show any dislocations along the rows in the [$\bar{1}$10] direction.

The regularity evident in the structure of Fig. 6 has been investigated in a series of topographs taken side by side by shifting the x position of the tunneling tip by the topograph width. The pattern of Fig. 6 was repeated over a studied region approximately 1 μm wide with remarkable consistency, revealing a surface "striping" effect with alternate stripes of the order of 0.1 μm in width. Figure 7(a) shows a combination of topographs which can be roughly laid end to end, tracking across the sample surface at ~45° [see schematic in Fig. 7(b)], with the dark areas corresponding to stepped regions and the lighter areas corresponding to the saturated terraces of the 5×2 reconstruction. Analysis of such topographs gave the average width of the 5×2 terrace as 730±100 Å, while the width of the intervening step regions was mea-

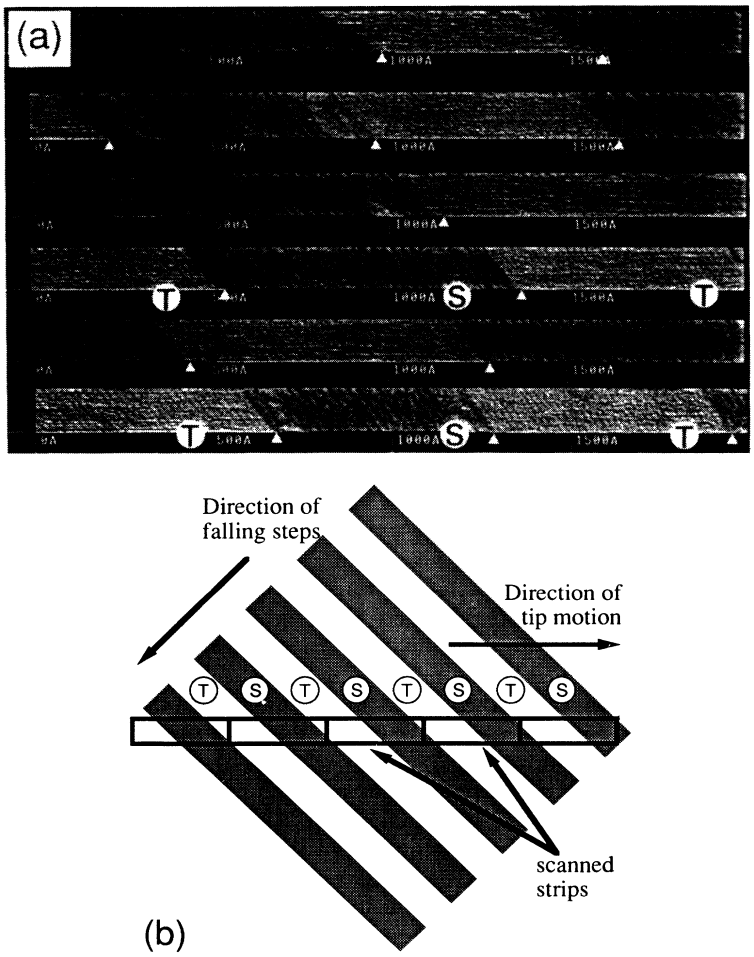

FIG. 7. (a) A series of topographs, each 2000 Å wide, of the Si surface saturated with the Au-induced 5×2 reconstruction, taken by moving the tunneling tip along the sample in steps of approximately 2000 Å, as indicated in the schematic (b). All strips were equivalently imaged. The strips, when roughly placed end to end, give an overall scan width of >1 μm across the sample surface at ~45° to the step normal direction. Stepped regions (S) and 5×2 terraces (T) are indicated on the schematic and on some topographs. Each boundary between regions is indicated by an arrowhead on the topographs.

sured as 880±100 Å, giving a ratio of terrace region width to stepped region width of 0.8±0.2. Together with the verified cutoff angle of the initial substrate from the (111) surface,[35] this ratio implies that the facet plane in the stepped regions is required to have an average misorientation angle with respect to the [111] normal of 7.50±1.0°, in order to maintain the average offcut. This expectation was verified by direct STM measurement in the stepped regions.

Figure 8 reveals the detail of the step regions at saturation coverage for the 5×2 structure. The average step separation measured was 21±1 Å, close to half that measured on the original clean Si substrate. This distance is slightly smaller than the 23.3 Å required to accommodate a 7×7 unit, but larger than the 16.6 Å needed for the 5×2 unit. Assuming the ideal single step height on the (111) surface of 3.135 Å, the angle at which the facet is oriented with respect to the [111] direction is calculated as 8.5°. Direct assessment of step heights found values slightly less than the ideal, reducing this angle to 8.1°, all in agreement with the facet angle obtained from analysis of macroscopic region widths in Fig. 7. The facet plane normal in the step regions is approximately along [775].

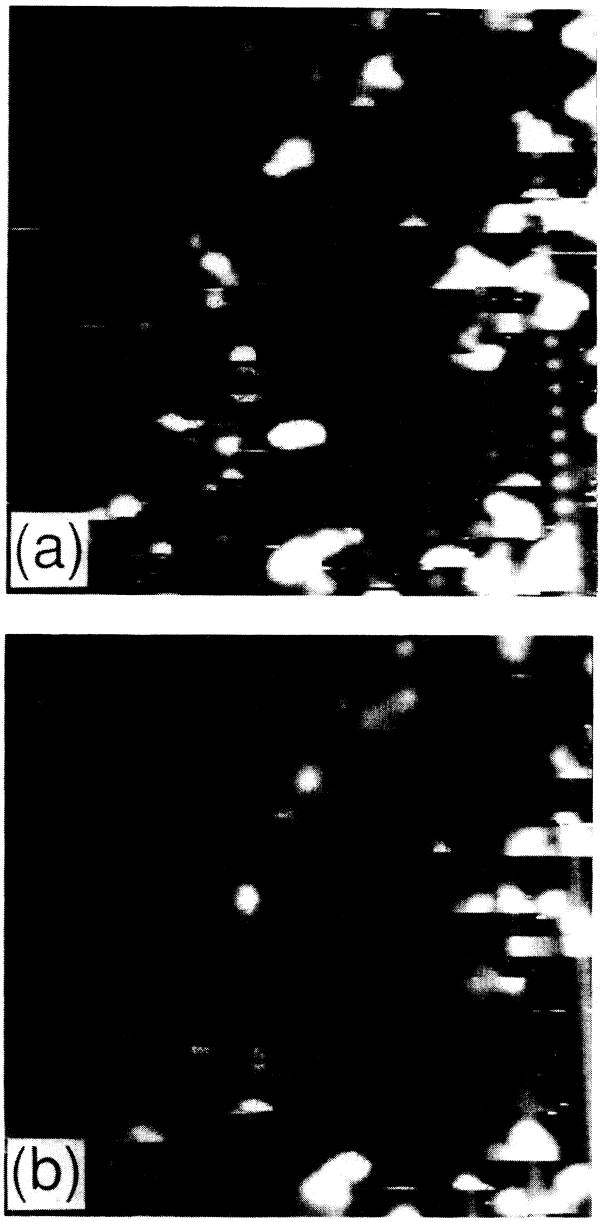

FIG. 8. The stepped regions, as seen when there is a saturation coverage of the Au-induced 5×2 reconstruction on the terraces: (a) A 200 Å×200 Å topograph taken at +2 V sample bias and 1 nA tunneling current. Strings of localized features decorate the step edges in the [$\bar{1}$10] direction. The features do not line up from string to string along the step normal, but are shifted. (b) The same area when viewed at reverse sample bias. The edge features now appear to form a continuous line.

Closer examination of the stepped regions in Fig. 8 reveals that the step edges are decorated with bright lines of features at $2a$ intervals. There is sometimes a fault where the step separation reduces slightly, leading to no relative phase shift between the bright features on the edges bounding this shorter terrace. This pattern is similar to that found at the boundary between 7×7 and 5×2 regions for smaller coverages of Au, as seen in Figs. 3(a) and 5. This provides further evidence that a step exists at the boundary of the 7×7 and 5×2 regions at lower coverage. The features are only resolved when empty electronic states are probed, as shown in Fig. 8(a), while probing filled states reveals a continuous step edge structure [Fig. 8(b)]. This step decoration was only found at saturation coverage of the 5×2 structure. The edge features of Fig. 8(a) do not line up from row to row, but are generally incoherent in the [$\bar{1}$10] direction by $\pm a/2$. Single height steps on an ideal Si(111) surface, when separated by the step-step distance of 21±1 Å observed in Fig. 8, have a phase shift of $\pm a/2$ in their edge features.

IV. DISCUSSION

A. The Si(111)-5×2-Au structure

The transition line between the 7×7 and 5×2 regions appears to consist of dimers spaced at $2a$ along the [$\bar{1}$10] direction. From such topographs, where the 7×7 is visible, it is possible to determine the registry of the observed features with respect to the underlying Si lattice. The more sharply defined structures evident in the filled states topographs of Figs. 3(a) and 4 allow for more detailed analysis than for the empty states. The measured positions of the main features are shown in Fig. 9, with appropriate correction for thermal drift. The ideal Si(111) structure is represented by a series of shaded hexagons depicting the bulk bilayer structure, with the black dots representing the upper atoms in the bilayer. This corresponds to the first ideal bilayer underlying the Si(111)7×7 reconstruction.[36] Figure 9 shows that the labeled features of Fig. 4 are not restrained to one particular type of site, consistent with the model-independent x-ray standing-wave analysis of Berman, Batterman, and Blakely.[15] The positioning of the labeled features of Fig. 4 on an ideal Si(111) lattice of Fig. 9 should not be taken to imply that a simple ideal Si(111) structure underlies the 5×2 reconstruction. Neither does it imply that these are *atomic* positions, since the density-of-states STM im-

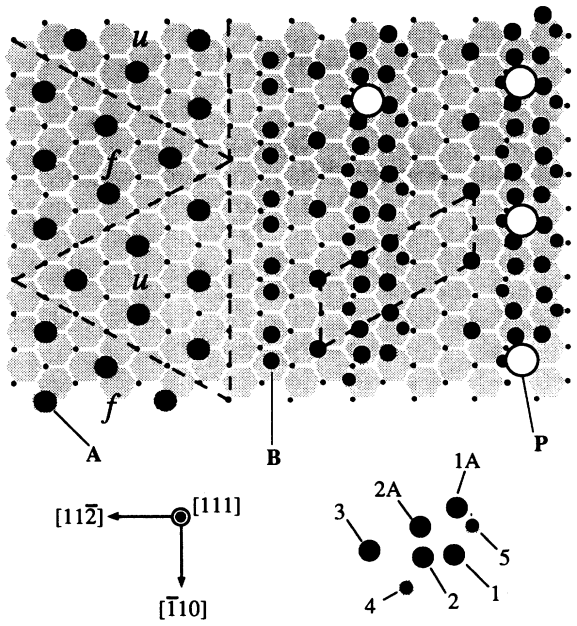

FIG. 9. The registry of the filled states features in the 5×2 unit, together with the adatom positions of the faulted (f) and unfaulted (u) halves of the 7×7 reconstruction, and the boundary features. The positions have been derived from images such as Figs. 2–5, with appropriate corrections for thermal drift. The ideal Si(111) surface is represented by a series of hexagons, as described in the text.

age may be somewhat removed from the core positions, as demonstrated recently, for example, by the work of Ding, Chan, and Ho[37] on the Si(111)-Ag system. The derived registry places many of the 5×2 features (1, 1A, 2, 3, 5) over "up" atoms of the ideal underlayer, if the entire 7×7 is considered to be removed on Au adsorption. If the 7×7 is, on the other hand, reconstructed into an ideal bilayer, then these features sit in "hollow" sites, which is intuitively more appealing. The REM work discussed above,[5,16,20] as well as recent STM studies,[28] has indicated substantial mobility of Si atoms in this system on Au deposition, and the large-scale topographical changes reported here support that view.

Recent STM studies of the 5×2 structure,[18,26] though of lower resolution, revealed a complex topography, comprising round, rectangular, and triangular units, and also the bright "protrusions."[18] Figure 3 of Ref. 18 reports three main features, A, B, and C, observed by their STM. Their round feature A can now be identified with feature 3 in our Fig. 4, the tail of the Y. Their rectangular feature B is an unresolved image of the arms of a single Y unit (features 1, 1A, 2, 2A of our Fig. 4) and their triangular feature C is now shown to consist of the arms of adjacent Y units. The recent x-ray diffraction study by Schamper *et al.*[25] of this structure produced a number of different possible arrangements of Au atoms on a slightly perturbed ideal Si(111) lattice. One model in particular bore a striking resemblance to the Y structure of Fig. 4. However, the x-ray diffraction work has to contend with complications arising from the presence of three domains of the 5×2 structure and comparison with Fig. 4 here shows that too high a symmetry may have been assumed in their analysis.

The Au coverage constraints must also be considered. Precision measurements reported by Bauer[24] of the coverage ratio of the saturated 5×2 phase to the $\sqrt{3}\times\sqrt{3}R\,30°$ phase gave a value of 0.665±0.010. The coverage value for the $\sqrt{3}\times\sqrt{3}R\,30°$ phase is disputed, and is generally reported as either $\frac{2}{3}$ or 1 ML. Assuming, as Bauer does,[24] a coverage of $\frac{2}{3}$ ML at saturation for the $\sqrt{3}\times\sqrt{3}R\,30°$ phase, the 5×2 coverage can then be calculated as 0.443±0.008 ML. This implies an average of 4.5 Au atoms per 5×2 unit cell, so it is clear in this case that not all of the labeled features in Fig. 4 could arise from Au atoms. The location of feature P in sites at 4a intervals gives it an occupancy in the 5×2 cells of 0.5, which could account for half-integer values of the coverage figure if it was considered due to a Au atom. The Y-shaped cluster of Schamper *et al.*,[25] however, consists entirely of Au atoms, requiring fractional occupation of Au sites to maintain consistency with this coverage. The uniformity of structure presented in Fig. 4 makes such fractional occupancy highly unlikely. However, when a coverage of 1 ML is assumed for the $\sqrt{3}\times\sqrt{3}R\,30°$ phase, then the 5×2 coverage works out, using Bauer's ratio,[34] as 0.665±0.010 ML. This is close to 7 Au atoms per unit cell, and could correspond to the seven main features we observe in Fig. 4.

Figure 4 indicates a structure which sharply contrasts with the simplicity of the models presented for this phase to date. There is an intriguing slight, but definite, asymmetry in the Y units about the [11$\bar{2}$] step normal, despite the existence of a mirror plane in this direction on the clean substrate. This is clear from Figs. 3 and 4. This asymmetry cannot be explained by thermal drift alone, but it is not possible to exclude tip effects in the imaging in this single domain system. There is a strong regularity in the row structure, and no dislocations along the rows in the [$\bar{1}$10] direction were observed, despite the local irregularity of the initial steps on the clean vicinal Si surface. This fact, along with observation of Figs. 2 and 6, shows that the initial stages of nucleation and growth are localized to the step-edge area. The continuity along the step edges confirms earlier studies[5,16,28] that growth is strongest along the 2× direction, and proceeds in a row by row fashion, leading to the abrupt discontinuity between the 7×7 and 5×2 structures.

B. The mesoscopic structure

The saturation surface structure of Fig. 7 indicates a system which has undergone a reorganization over mesoscopic distances. Figure 10 illustrates, schematically, the changing mesoscopic structure observed with increasing Au coverage. It is clear that a complete reorganizing of the structure must occur with each deposition. The mobility of both Si *and* Au atoms on the surface must be high for this to occur. Evidence for Au diffusion on Si surfaces at rates of the order of 1 μm s^{-1} has been reported previously in the temperature range used here.[17] The transformation of the 5×2 to a 1×1 at temperatures close to those used for deposition provides

additional indications of high mobility.

Previous studies have shown that short annealings of the clean vicinal surface represented by Fig. 1, at temperatures near 600 °C, did not change the step-edge structure significantly.[35] Thus, the immediate increased ordering of the step edges found with 0.1 ML of Au deposition must be due to the influence of the Au. This increased ordering occurs though no direct evidence was found of Au presence at the step edges. Given the high mobility of Au and Si atoms necessary to form the mesoscopic structure at the deposition temperature used here, and the small energy differences associated with stepped Si structures,[38] it is suggested that the Au, while diffusing over the surface in search of the 5×2 structure, has a significant residence time in the region of the steps where a 5×2 structure does *not* grow at that coverage. While the nucleation of the 5×2 structure at steps shows that the Au binds preferentially to steps rather than terrace, the mesoscopic structure shows that the most strongly bound state for the Au is the 5×2. Further evidence for this comes from our Au desorption studies, where the

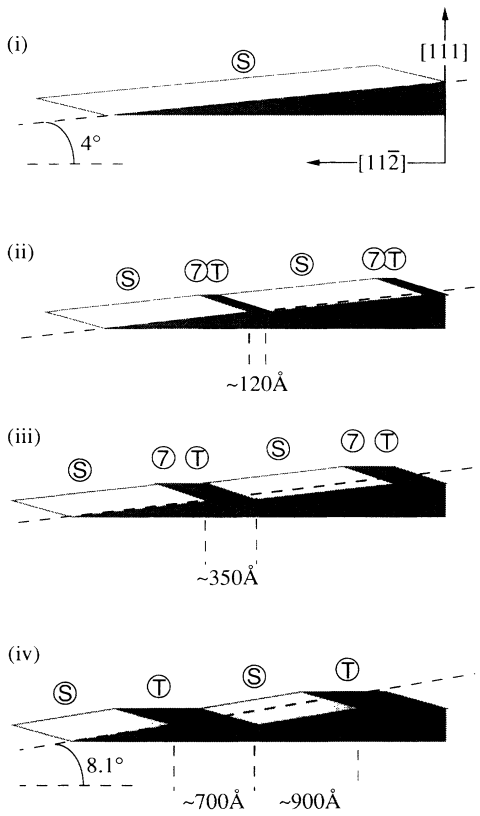

FIG. 10. The macroscopic surface structure illustrated schematically for (i) clean vicinal Si(111), (ii) 0.1-ML Au deposition, (iii) 0.2-ML Au deposition, and (iv) saturation of the 5×2 phase. The facet angle increases with Au coverage from the initial clean 4° offcut to the saturation 8.1°. Step regions are indicated by (*S*), 7×7 terrace regions by (7), and 5×2 terrace areas by (*T*). The overall 4° misorientation is maintained by the growth of the flat terrace regions, interleaved with the step regions. These terraces first appear composite, exhibiting 5×2 and 7×7 structures, and later are saturated by the 5×2 reconstruction.

higher 6×6 and $\sqrt{3}\times\sqrt{3}R30°$ structures desorb at significantly lower temperatures than the 5×2. In addition, the step decoration features only seen at saturation coverage (Fig. 8) would be consistent with the view that the Au atoms are more strongly bound in the 5×2 structure than at the steps, if the features observed are due to Au atoms at the step edges when the 5×2 regions are saturated. Also the regularity of both the step edge structures in Fig. 8 and the 5×2 row structures themselves may make them suitable candidates for quantum-wire effects. The presence of Au at the steps may, even for a short time, catalyze their reordering and straightening. Temperature-dependent STM studies are necessary to investigate this hypothesis. Earlier STM studies[26] may have indicated a catalytic effect, as they revealed a tendency for the Si(111) substrate itself to adopt a 5× periodicity in the presence of very small quantities of Au. This restructuring is seen in Fig. 2(b).

Regarding the detail of the growth, Figs. 2 and 5 show that the presence of the 5×2 structure has facilitated the reconstruction of the step region below it into a 7×7 terrace, while it grows into the rising step edge. The initial increase in the size of the 7×7 regions seen in Fig. 2 confirms this. The comparable widths of the 5×2 and 7×7 regions in Fig. 2, and at higher Au coverages prior to saturation, are consistent with growth of the Au-induced 5×2 terrace regions on both sides of the nucleation step, releasing extra Si atoms from the consumed upper steps that diffuse to the lower steps and fill them in, forming a 7×7 terrace. This has been previously postulated from REM and STM studies of Au growth on the singular Si(111) surface.[20,28] The advantage of the vicinal surface here is that the initial uniform step distribution allows a clear distinction to be made between 7×7 terrace growth above and below the 5×2 terrace growth. The fact that large terraces of 7×7 can be formed while 5×2 terraces are still increasing shows that the Au is more strongly inclined to complete existing 5×2 regions than to randomly attack 7×7 adatoms or dangling bonds.

No fully quantitative growth model will be attempted here. However, the approximately equal areas of 7×7 and 5×2 structures on the terraces at intermediate coverages are consistent with roughly equal rates of growth above and below the nucleation step, assuming Tanishiro and Takayanagi's estimate of about 40% of the surface Si atoms being displaced from the 5×2 regions.[16] If 50% of the surface Si atoms move from the below-step region, where half the growth occurs, and the other half of the growth above consumes the upper step, thus releasing 150% of the surface Si atoms, then in total 100% of the Si atoms are displaced to grow more 7×7 terrace area, equalizing with the 5×2 terrace formed in the process. This simultaneous expansion both above and below the nucleation site at the step edge has indeed been observed recently by STM.[28] The stepped regions also appear to respond to the Au deposition at 600 °C, and it is possible that the Au catalyzes facet formation that is known to be favored below 850 °C,[39] but which is avoided on the clean substrate in this work by quenching the high-temperature structure.[35]

V. CONCLUSIONS

The nucleation of Au at step edges on vicinal Si(111) leads to the growth of single domain Si(111)-5×2-Au, initially coexisting with the Si(111)-7×7 reconstruction. The approximately equal areas of 5×2 and 7×7 terraces found at coverages below saturation indicate growth both away from and into the nucleation step, if about half the Si surface atoms are removed in forming the 5×2 structure. Further, this work reveals gradual changes in local facet angle on the vicinal Si surface, driven by terrace growth of the 5×2 structure. Sharp boundaries between the 5×2 and 7×7 reconstructions, and with the stepped regions, were followed as Au growth progressed, and the detailed structure of the step and 5×2 regions was presented. Long diffusion lengths lead to mesoscopic structure and a nonuniform Au coverage at saturation for the 5×2, with a pattern extending over distances on the order of micrometers. Of particular interest is the regularity of both the 5×2 rows and the step decoration features within the faceted regions at saturation coverage. These may function as quantum wires and are currently under closer investigation.

The vicinal offcut has simplified some of the problems of the Si(111)-5×2-Au structure by restraining the growth direction and reducing the overlayer symmetry. Despite this, however, atomic resolution images of the overlayer reconstruction, the phase boundaries, and the facet-region structure indicate that considerable complexity remains in this system. Further work on the single domain system is required, with all techniques, particularly with respect to the vertical registry of the Au atoms involved in the formation of the 5×2 structure. Both temperature-dependent STM studies and single domain surface x-ray diffraction studies appear to be particularly promising.

ACKNOWLEDGMENTS

This research was supported by the CEC SCIENCE programme. J.D.O'M. would like to acknowledge discussions with Dr. I. R. Collins, Dr. R. Cosso, and Dr. C. H. Patterson.

*To whom correspondence should be addressed.
†Present address: Physics Department, Technical University of Eindhoven, 5600MB Eindhoven, Holland.

[1]J. J. Lander, Surf. Sci. **1**, 125 (1964).
[2]H. E. Bishop and J. C. Rivière, J. Phys. D **2**, 1635 (1969).
[3]H. Lipson and K. E. Singer, J. Phys. C **7**, 12 (1974).
[4]G. Le Lay and J. P. Faurie, Surf. Sci. **69**, 295 (1977).
[5]N. Osakabe, Y. Tanishiro, K. Yagi, and G. Honjo, Surf. Sci. **97**, 393 (1980).
[6]P. Perfetti, S. Nannarone, F. Patella, C. Quaresima, M. Capozi, A. Savoia, and G. Ottaviani, Phys. Rev. B **26**, 1125 (1982).
[7]Y. Yabuuchi, F. Shoji, K. Oura, and T. Hanawa, Surf. Sci. **131**, L411 (1983).
[8]G. Le Lay, Surf. Sci. **132**, 169 (1983).
[9]K. Oura, M. Katayama, F. Shoji, and T. Hanawa, Phys. Rev. Lett. **55**, 1486 (1985).
[10]M. Ichikawa, T. Doi, and K. Hayakawa, Surf. Sci. **159**, 133 (1985).
[11]F. Salvan, H. Fuchs, A. Baratoff, and G. Binnig, Surf. Sci. **162**, 634 (1985).
[12]J. F. McGilp and Y. Yeh, Solid State Commun. **59**, 91 (1986).
[13]J. F. McGilp, Semicond. Sci. Technol. **2**, 102 (1987).
[14]J. H. Huang and R. S. Williams, Surf. Sci. **204**, 445 (1988).
[15]L. E. Berman, B. W. Batterman, and J. M. Blakely, Phys. Rev. B **38**, 5397 (1988).
[16]Y. Tanishiro and K. Takayanagi, Ultramicrosc. **31**, 20 (1989).
[17]T. Ichinokawa, I. Hamaguchi, M. Hibino, and J. Kirschner, Surf. Sci. **209**, L144 (1989).
[18]A. A. Baski, J. Nogami, and C. F. Quate, Phys. Rev. B **41**, 10 247 (1990).
[19]C. J. Karlsson, E. Landemark, L. S. O. Johansson, and R. I. G. Uhrberg, Phys. Rev. B **42**, 9546 (1990).
[20]Y. Tanishiro, K. Yagi, and K. Takayanagi, Surf. Sci. **234**, 37 (1990).
[21]H. Daimon, C. Chung, S. Ino, and Y. Watanabe, Surf. Sci. **235**, 142 (1990).
[22]T. Hasegawa, K. Takata, S. Hosaka, and S. Hosoki, J. Vac. Sci. Technol. A **8**, 241 (1990).
[23]S. Takahashi, Y. Tanishiro, and K. Takayanagi, Surf. Sci. **242**, 73 (1991).
[24]E. Bauer, Surf. Sci. Lett. **250**, L379 (1991).
[25]Ch. Schamper, W. Moritz, H. Schulz, R. Feidenhans'l, M. Neilsen, F. Grey, and R. L. Johnson, Phys. Rev. B **43**, 12 130 (1991).
[26]T. Hasegawa, K. Takata, S. Hosaka, and S. Hosoki, J. Vac. Sci. Technol. B **9**, 758 (1991).
[27]J. D. O'Mahony, P. V. Kelly, and J. F. McGilp, Appl. Surf. Sci. **56-58**, 449 (1992).
[28]T. Hasegawa, S. Hosaka, and S. Hosoki, Jpn. J. Appl. Phys. **31**, L1492 (1992).
[29]S. Hasegawa and S. Ino, Phys. Rev. Lett. **68**, 1192 (1992).
[30]J. D. O'Mahony, C. H. Patterson, J. F. McGilp, F. M. Leibsle, P. Weightman, and C. F. J. Flipse, Surf. Sci. Lett. **277**, L57 (1992).
[31]J. D. O'Mahony, J. F. McGilp, M. H. W. Verbruggen, and C. F. J. Flipse, Surf. Sci. **287/288**, 713 (1993).
[32]N. C. Bartelt, E. D. Williams, R. J. Phaneuf, Y. Yang, and S. Das Sarma, J. Vac. Sci. Technol. A **7**, 1898 (1989).
[33]M. W. Geis, D. C. Flanders, and H. I. Smith, Appl. Phys. Lett. **35**, 71 (1979).
[34]K. Yagi, J. Appl. Crystallogr. **20**, 147 (1987).
[35]J. D. O'Mahony, J. F. McGilp, F. M. Leibsle, P. Weightman, and C. F. J. Flipse, Semicond. Sci. Technol. **8**, 495 (1993).
[36]K. Takayanagi, Y. Tanishiro, M. Takahashi, and S. Takahashi, J. Vac. Sci. Technol. A **3**, 1502 (1985); Surf. Sci. **164**, 367 (1985).
[37]Y. G. Ding, C. T. Chang, and K. M. Ho, Phys. Rev. Lett. **67**, 1454 (1985).
[38]E. D. Williams and N. C. Bartelt, Ultramicrosc. **31**, 36 (1989), and references therein.
[39]J. L. Goldberg, X.-S. Wang, J. Wei, N. C. Bartelt, and E. D. Williams, J. Vac. Sci. Technol. A **9**, 1868 (1991).

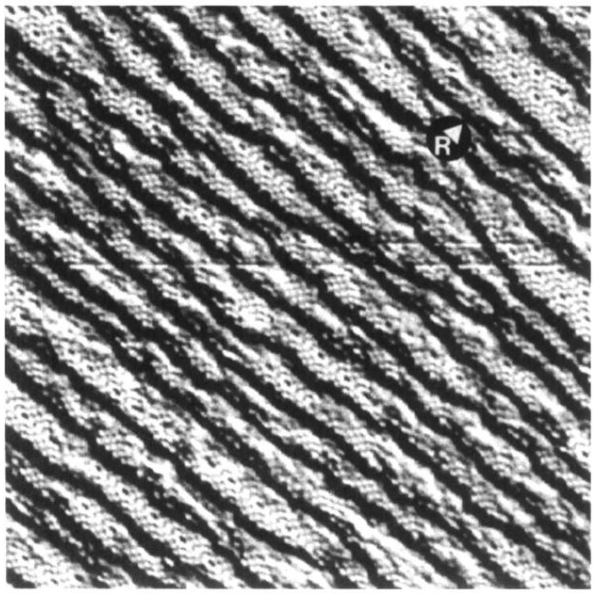

FIG. 1. A 600 Å $\times$ 600 Å STM topograph of a vicinal Si(111) cut 4° off the [111] towards [11$\bar{2}$]. The surface was produced by flashing the sample twice to 1280 °C for 20 s, followed by quench cooling (Ref. 35). The arrow, labeled *R*, indicates rising step edges in the [$\bar{1}\,\bar{1}\,2$] direction. The tunneling current was 1 nA for a sample bias of +2 V. The image is nine point smoothed and differentiated to highlight the step edges.

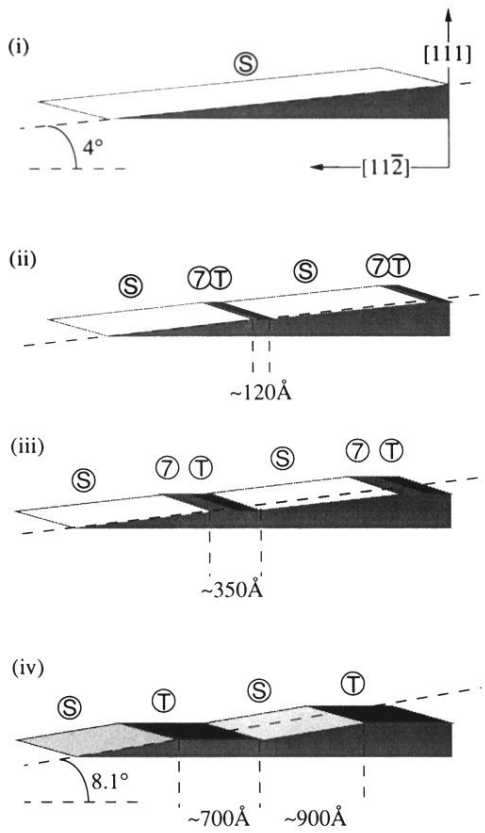

FIG. 10. The macroscopic surface structure illustrated schematically for (i) clean vicinal Si(111), (ii) 0.1-ML Au deposition, (iii) 0.2-ML Au deposition, and (iv) saturation of the 5×2 phase. The facet angle increases with Au coverage from the initial clean 4° offcut to the saturation 8.1°. Step regions are indicated by (*S*), 7×7 terrace regions by (7), and 5×2 terrace areas by (*T*). The overall 4° misorientation is maintained by the growth of the flat terrace regions, interleaved with the step regions. These terraces first appear composite, exhibiting 5×2 and 7×7 structures, and later are saturated by the 5×2 reconstruction.

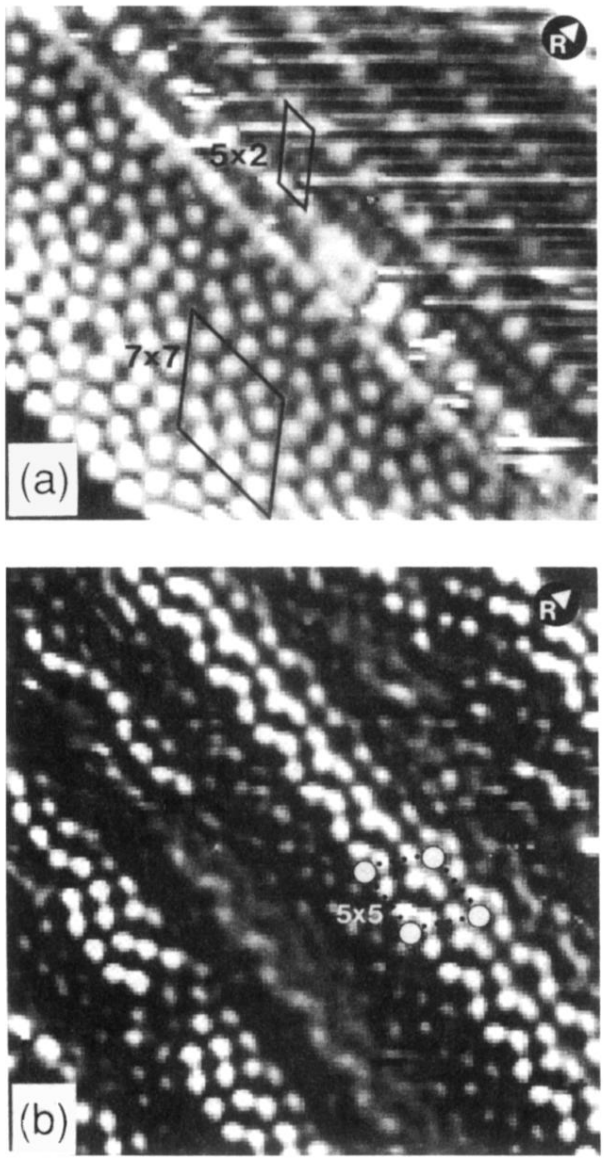

FIG. 2. (a) 120 Å × 140 Å STM topograph of a small composite terrace of 7×7 and 5×2 reconstructions found after an initial deposition of 0.1 ML of Au, as detailed in the text. The unit cells are indicated. The two reconstructed regions share a sharp boundary in the $[\bar{1}10]$ direction. The tunneling current was 1 nA for a sample bias of +2 V. (b) Enhanced step-edge ordering after initial deposition of ~0.1 ML of Au under the tunneling conditions used in (a). At step edges, small regions of the 5×5 reconstruction can now be found. The step edges run through the corner holes in the $[\bar{1}10]$ direction. *R* indicates the rising step-edge direction.

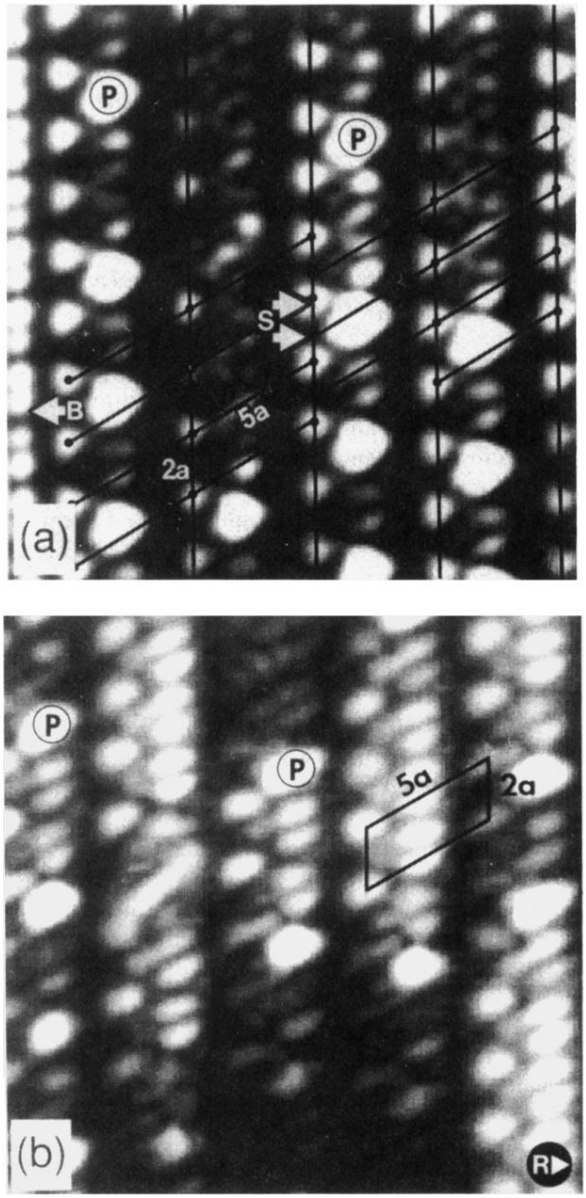

FIG. 3. (a) An 80-Å-square STM topograph taken at −0.4 V sample bias and 1.2 nA tunneling current showing the single domain 5×2 Au-induced reconstruction on Si(111). The slippage of rows (Ref. 3) is indicated by *S*. Large bright areas, termed "protrusions" (Ref. 18) and labeled *P*, occur at sites spaced no closer than 4*a* in the [$\bar{1}$10] direction [*a* is 3.84 Å on the Si(111) surface]. The boundary line between the 5×2 and 7×7 reconstructions is indicated by *B*. (b) The same area as above imaged at sample bias +0.4 V and tunneling current 1.2 nA.

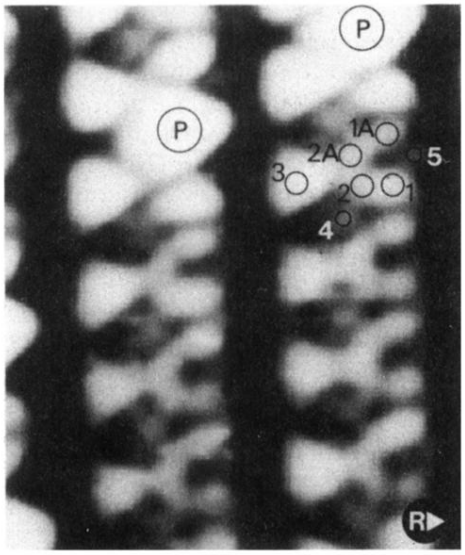

FIG. 4. A 35 Å×40 Å image of the slightly skewed Y structure unit seen in the filled states of the 5×2 rows. The topograph was taken at −0.4 V sample bias and 1.2 nA tunneling current. The main repeating features are labeled and *R* is the rising step-edge direction.

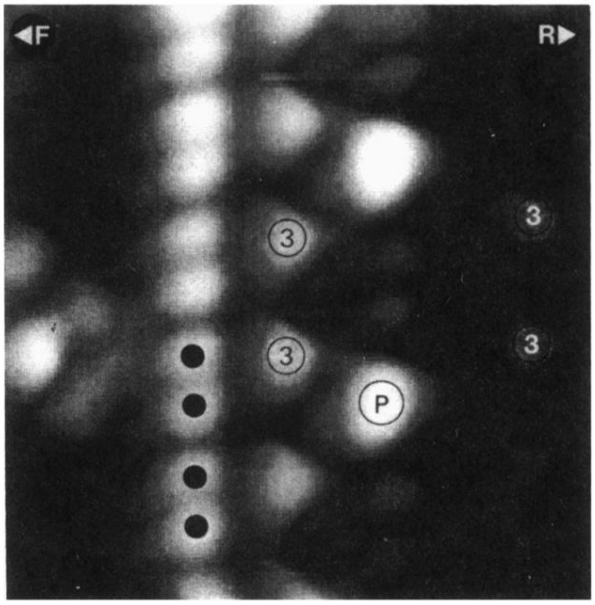

FIG. 5. The detail of the boundary area, shown here in a 40-Å-square image. The boundary line itself is indicated with black dots. These structures appear to be dimerized. The dimer centers are spaced $2a$ apart, the distance between two tail features (3) as labeled in Fig. 4. Rising and falling step-edge directions are indicated, as is a protrusion feature. This image, measured at 1.2 nA and -0.4 V sample bias, has been differentiated to highlight the main features of interest.

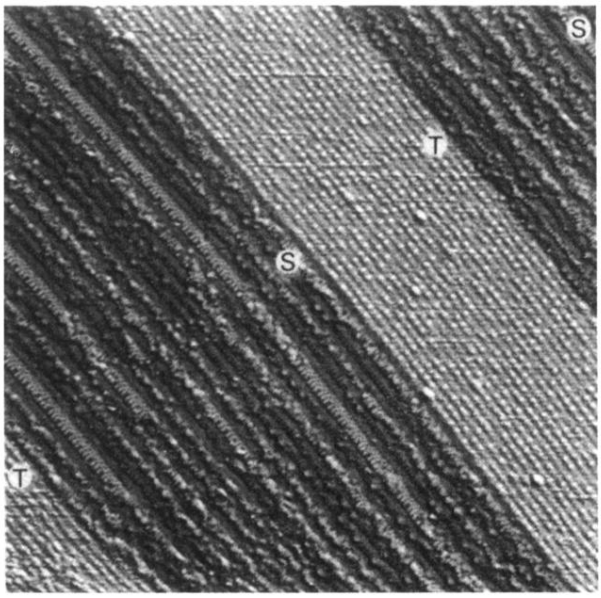

FIG. 6. A topograph measuring 1000 Å square showing a surface with regular saturated terraces (T) consisting only of the 5×2 reconstruction, separated by stepped regions (S). The boundary between these regions along the $[\bar{1}10]$ direction is seen to be very regular and sharp. The image has been differentiated and nine-point smoothed.

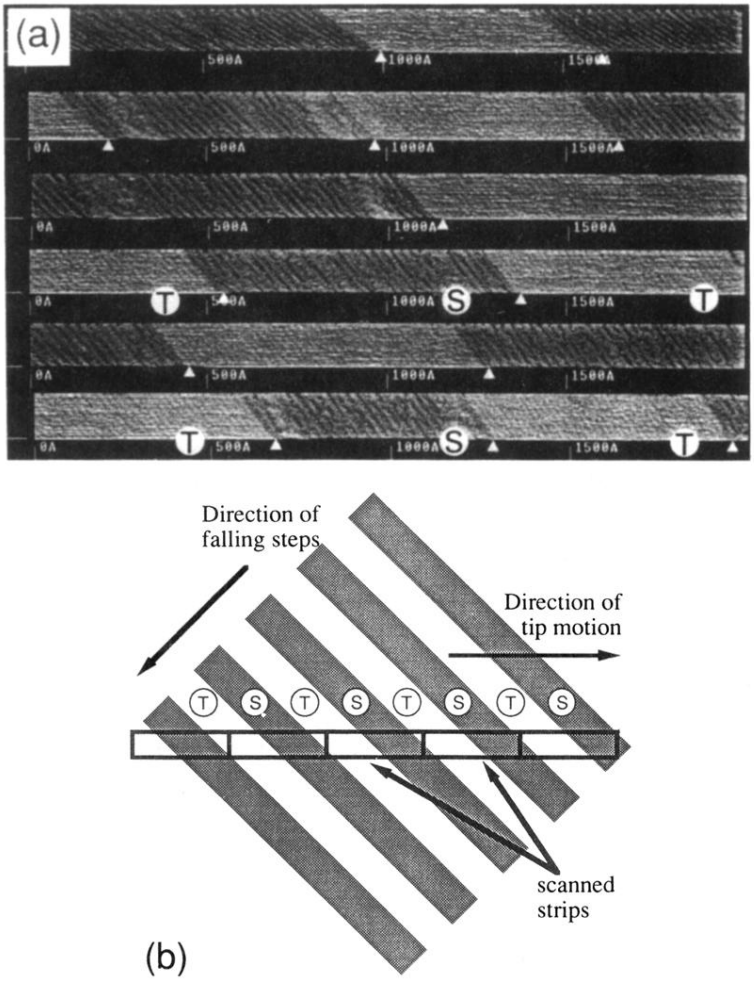

FIG. 7. (a) A series of topographs, each 2000 Å wide, of the Si surface saturated with the Au-induced 5×2 reconstruction, taken by moving the tunneling tip along the sample in steps of approximately 2000 Å, as indicated in the schematic (b). All strips were equivalently imaged. The strips, when roughly placed end to end, give an overall scan width of >1 μm across the sample surface at $\sim45°$ to the step normal direction. Stepped regions (S) and 5×2 terraces (T) are indicated on the schematic and on some topographs. Each boundary between regions is indicated by an arrowhead on the topographs.

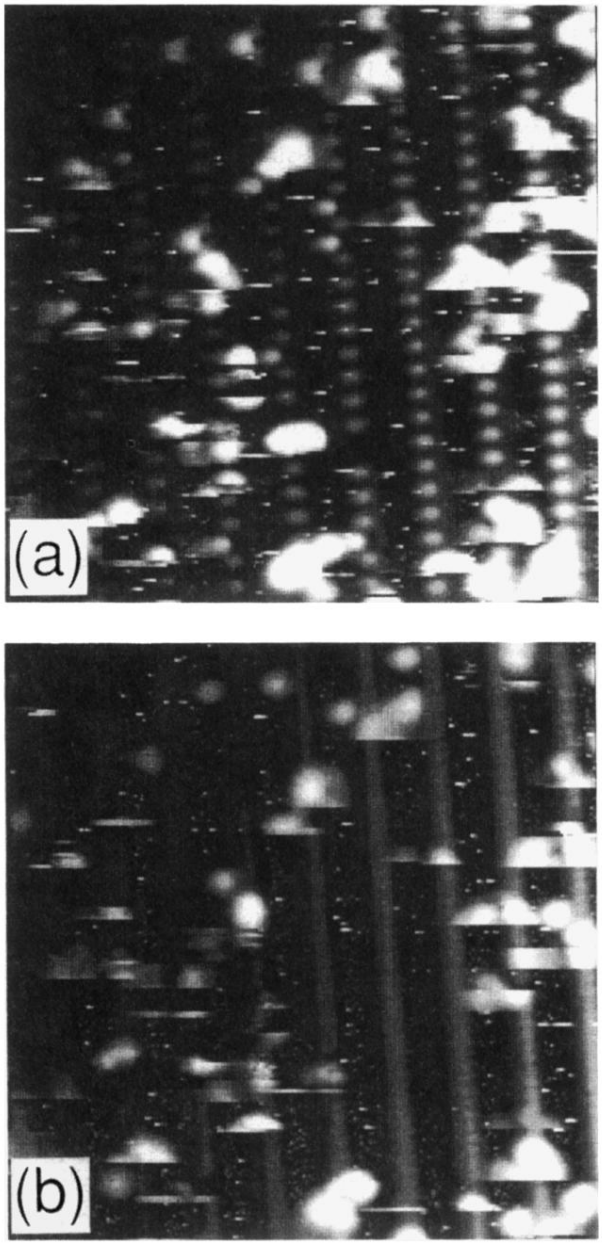

FIG. 8. The stepped regions, as seen when there is a saturation coverage of the Au-induced 5×2 reconstruction on the terraces: (a) A 200 Å$\times$200 Å topograph taken at $+2$ V sample bias and 1 nA tunneling current. Strings of localized features decorate the step edges in the $[\bar{1}10]$ direction. The features do not line up from string to string along the step normal, but are shifted. (b) The same area when viewed at reverse sample bias. The edge features now appear to form a continuous line.

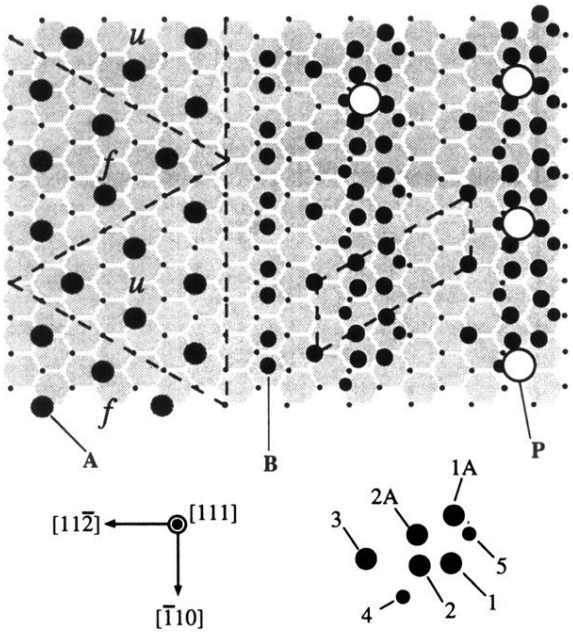

FIG. 9. The registry of the filled states features in the 5×2 unit, together with the adatom positions of the faulted (f) and unfaulted (u) halves of the 7×7 reconstruction, and the boundary features. The positions have been derived from images such as Figs. 2–5, with appropriate corrections for thermal drift. The ideal Si(111) surface is represented by a series of hexagons, as described in the text.